

Simulating the Power Output of Large Bifacial Photovoltaic Plants

Nikola Ostojić, Čedomir Zeljković, and Predrag Mršić

Faculty of Electrical Engineering, University of Banja Luka, Banja Luka, Bosnia and Herzegovina

E-mail address: ostojic_n@live.com, cedomir.zeljkovic@etf.unibl.org, predrag.mrsic@etf.unibl.org

Abstract—Bifacial photovoltaic modules have gained increasing attention in the last decade due to their potential to achieve higher annual energy yield in comparison to conventional monofacial modules. Since the higher energy production is also accompanied by higher investment costs, it is necessary to conduct a careful techno-economic analysis in order to provide the investors an answer about their accurate cost efficiency. The achievable energy output of a bifacial photovoltaic power plant is influenced by many factors such as module geometry, row spacing, orientation of the modules and ground albedo. Since the methodology for prediction of the energy yield has not yet been standardized, the main target of this paper was to create one version of a comprehensive standalone energy calculator that would serve as a useful performance assessment tool for designers and investors. The developed software tool was tested on several characteristic scenarios and the obtained results were compared with the results provided by two freely available online calculators.

Keywords-Photovoltaic Power Plant, Bifacial PV Modules, View Factor

I. INTRODUCTION

Energy production using photovoltaic (PV) systems has become increasingly attractive in the last decade, primarily thanks to the development of technology and falling prices. Cumulative PV capacity has reached the global total of about 627 GW in 2019 which is a tremendous progress in comparison to the capacity of 23 GW observed ten years back in 2009 [1]. Photovoltaic conversion shows a number of good features such as direct energy transformation from solar radiation to direct current without rotating parts, noise and vibration. On the other hand, photovoltaic technology is characterized by the occupation of large areas of land per unit of installed power, so their use is limited by other competitive land uses, such as agriculture, forestry, nature conservation, and urban infrastructure [2]. One way to increase the energy yield of photovoltaic power plants is to use bifacial solar panels, which are capable of collecting solar radiation falling both on their front and rear side. Although the first industrial bifacial photovoltaic modules date back to the 1980s, their application in practice has intensified over the last ten years [3]. The world first large scale 1.25 MW bifacial PV power plant, which is built on snowy area in Asahikawa Japan, produced about 20% more energy in comparison to its monofacial counterpart during the first three years of operation [4]. According to predictions published in IRPTV report, the bifacial PV market share of about 20% observed in 2020 is expected to increase significantly to 70% within the next 10 years [5].

There are a number of papers that examine different aspects of bifacial PV plants. Cuevas et al. were the first to claim that bifacial panels under certain circumstances are capable of

giving up to 50% more energy than conventional monofacial panels [6]. However, this was just a special case, because studies and practice show different results. It was necessary to develop detailed models for precise estimation of power output achievable by real bifacial PV plants. Primarily, the optical models are needed for computing the irradiation on PV modules, considering the influence of adjacent modules and other obstacles. A valuable contribution to the development of so-called optical view factors is made by Appelbaum [7][8]. These models have been further refined by other authors, such as Durković and Đurišić [9] and Chudinow et al. [10]. Along with the optical models, the electrical and thermal models have been concurrently developed. Some of the most common electrical models include the single-point power model [11], characteristic point model [12] and various equivalent circuit models [13]. Well-known thermal models are the Sandia model [14], NOCT model [15], and Faiman (or PVSyst) model [16].

The goal of this paper is selecting and integration of required models into a comprehensive software tool for simulation and estimation of energy output of large bifacial PV plants. The mathematical models are implemented as MATLAB/Octave program routines and the developed software is tested on the potential PV plant built near Banja Luka, Bosnia and Herzegovina. The impact of several important input variables is examined including the module tilt angle, the distance between the rows and the ground albedo.

II. SIMULATION METHODOLOGY

The performance of PV power plants is typically simulated by using the integration of three fundamental models, namely the optical model, thermal model and electrical model [13], [17]–[18]. The simulation framework established in this paper

is also based on such three models, fed by the appropriate input variables and parameters, as presented in Fig. 1. Weather input parameters include direct normal irradiance (DNI), diffuse horizontal irradiance (DHI), ambient temperature (T_{amb}) and wind velocity (v_w), which can be obtained from some meteorological data companies. In our approach, these inputs are Typical Meteorological Year (TMY) hourly time series loaded from PVWatts online calculator [19]. Installation geometry parameters consist of module tilt angle (Σ), azimuth angle (Φ_C), elevation (E_p) and ground albedo (ρ). Astronomy model is responsible for finding the position of the Sun on the sky dome. The Sun position is represented by the altitude angle (β) and azimuth angle (Φ_S), which both continuously change depending on the time and date. Weather, astronomy and installation parameters are inputs for the optical model to calculate the front- and rear-side irradiances, which are combined with ambient temperature T_{amb} and wind velocity v_w in thermal model to obtain cell temperature T_c . The outputs of the optical model and thermal model are used as inputs to the electrical model, so that finally the PV system power output P_{AC} can be determined.

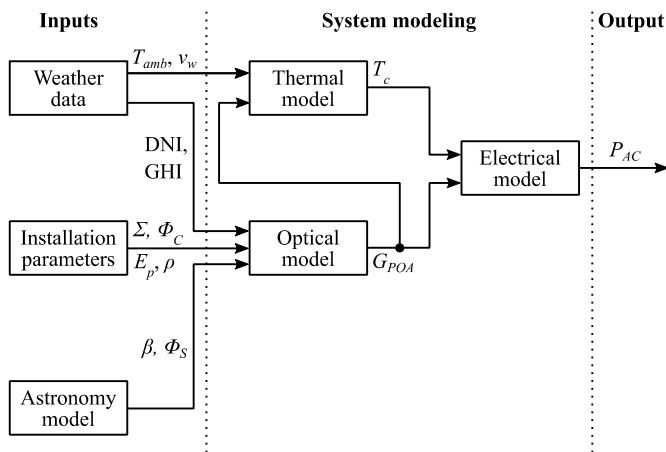


Figure 1. Basic components of the simulation framework

The main steps of the computational algorithm are as follows:

1. Load the input parameters
 - a. Load the location parameters
 - b. Load the weather parameters
 - c. Load the PV installation parameters
2. Repeat for each hour in a year
 - a. Determine the position of the sun on the sky
 - b. Determine the view factors
 - c. Determine the plane-of-array irradiance
 - d. Convert the irradiation into DC power
 - e. Convert the DC power into AC power
3. Find the annual totals
 - a. Compute the system annual energy output

III. MAIN MODELING ASPECTS

The most important modeling aspects used in the simulation framework are described in this section.

A. Solar Angles

Mathematical expressions for determining the position of the Sun on the sky are derived in many books [20][21]. In this approach, the following set of equations is used

$$\delta = 23,45 \cdot \sin \left[\frac{360}{365} \cdot (n - 81) \right] \quad (1)$$

$$\sin \beta = \cos L \cdot \cos \delta \cdot \cos \omega + \sin L \cdot \sin \delta \quad (2)$$

$$\omega = 15 \left[\frac{\circ}{h} \right] \cdot T_{usn} [h] \quad (3)$$

$$\sin \Phi_S = \frac{\cos \delta \cdot \sin \omega}{\cos \beta} \quad (4)$$

$$\cos \theta = \cos \beta \cdot \cos (\Phi_S - \Phi_C) \cdot \sin \Sigma + \sin \beta \cdot \cos \Sigma \quad (5)$$

where δ is the Sun declination angle, n is the day number, β is the Sun altitude angle, L is the latitude of the considered location, ω is the hour angle, T_{usn} is the time until the solar noon, Φ_S is the Sun azimuth angle, Φ_C is the collector azimuth angle, Σ is the collector tilt angle, and θ is the incidence angle.

B. Finding the Length of the Shadow on the Ground

When we look at several modules arranged side by side and in several rows, we can notice that behind each row of modules we have a surface that is shaded by the module itself and that this shaded area affects the radiation of both the back of the module that creates shadow (self-shading) and the front of the module located in the next row. From the shaded surface only diffuse radiation is reflected, while from the unshaded surface both direct and diffuse radiation are reflected. It is important to note that the shadow length is not constant, as it changes during the day depending on the position of the Sun. The position of the shadow depending on the PV module geometry is illustrated in Fig. 2.

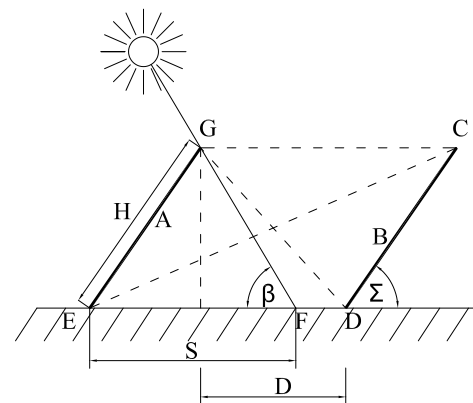


Figure 2. Panel Array Geometry

The length of the shadow S can be determined by using the following equation

$$S = H \cdot \cos \Sigma + H \cdot \sin \Sigma \cdot \frac{\cos (\Phi_S - \Phi_C)}{\tan \beta} \quad (6)$$

where H is the length of the module. Term $\cos(\Phi_S - \Phi_C)/\tan \beta$ essentially describes how the shadow length depends on the azimuth position of the Sun and azimuth orientation of PV modules, while the maximum possible length of the shadow on the ground area between the rows equals $(H \cdot \cos \Sigma + D)$.

C. The Role of View Factors

The general expression for calculating the irradiance on one arbitrary side of a bifacial photovoltaic module can be written in the following form

$$G_{1/2} = (1 - \varepsilon) \cdot G_b \cdot \cos \theta + F_{B \rightarrow sky} \cdot G_{dh} + \rho \cdot F_{B \rightarrow grd.us} \cdot G_h + \rho \cdot F_{B \rightarrow grd.s} \cdot G_{dh} \quad (7)$$

where ε is the coefficient describing the shading losses for direct irradiation due to modules from adjacent row, G_b is the direct irradiance on the normal surface, $F_{B \rightarrow sky}$ is the view factor of collector B to sky, G_{dh} is the diffuse irradiance on the horizontal surface, ρ is the ground albedo, $F_{B \rightarrow grd.us}$ is the view factor of collector B to unshaded ground, G_h is the global irradiance on a horizontal surface, and $F_{B \rightarrow grd.s}$ is the view factor of collector B to shaded ground. Irradiance on the other side of the module is also calculated by using equation (7), but taking into account certain specifics and differences, such as the level of direct radiation to the module as well as the appropriate view factors to sky and ground, which will be more clarified in section IIID.

View factors are obviously very important because they express the influence of PV modules from adjacent rows on blocking one part of the available radiation. The amount of the diffuse radiation on the collector depends on the view factor of the collector to sky, while the amount of reflected radiation on the collector depends on the view factor of the collector to ground. The logic for determining the view factors used in this paper is mainly based on the work of Appelbaum [8]. The basic principles for deriving necessary view factors are illustrated in Fig. 3.

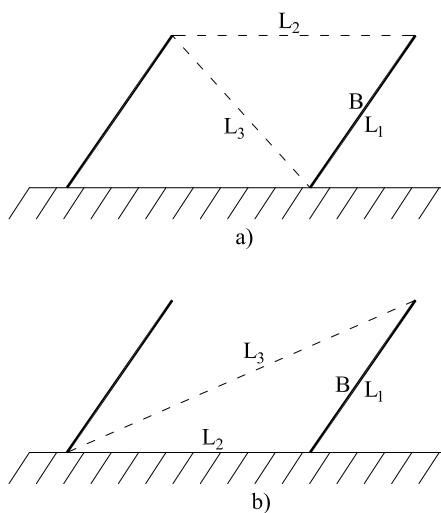


Figure 3. View factors: (a) to sky, and (b) to ground

The view factor of collector B to sky is determined by using the geometry parameters defined in Fig. 3a

$$F_{B \rightarrow sky} = \frac{L_1 + L_2 - L_3}{2 \cdot L_1} \quad (8)$$

The view factor of collector B to ground is calculated using practically the same expression

$$F_{B \rightarrow grd} = \frac{L_1 + L_2 - L_3}{2 \cdot L_1} \quad (9)$$

but now using the geometry parameters as defined in Fig. 3b.

D. View Factors for the Front Side of the Modules

1) Direct component

The principle for finding the view factor of collector B for direct beam radiation which is not blocked by adjacent collector A is illustrated in Fig 4. If collector B is not shaded then all available direct irradiance is utilized. If nevertheless some shading occurs, the available direct irradiance should be multiplied by $(1 - \varepsilon)$ in order to take into account the shading losses.

The length of the shadow S' cast on collector B can be calculated using the sine theorem

$$S' = \frac{\sin \beta}{\sin(180^\circ - \Sigma - \beta)} \cdot (S - H \cdot \cos \Sigma - D) \quad (10)$$

where S represents the length of the shadow on the ground, but which is not limited by the next row, as presented in Fig. 4.

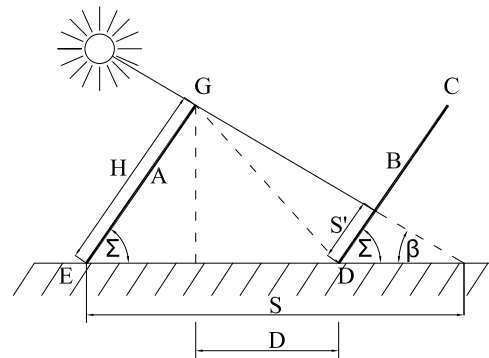


Figure 4. Length of the shadow S' on collector B cast by collector A

After determining the shadow length S' , the losses for the direct radiation component caused by the shading process can be calculated

$$\varepsilon = \frac{S'}{H} \quad (12)$$

2) Diffuse component

The view factor to sky of the front side of the collector B is calculated based on equation (8) and Fig. 2

$$L_1 = CD = H$$

$$L_2 = CG = D + H \cdot \cos \Sigma$$

$$L_3 = DG = \left[(H \cdot \sin \Sigma)^2 + D^2 \right]^{1/2}$$

from which it follows that

$$F_{B \rightarrow sky}^f = \frac{H + D + H \cdot \cos \Sigma - \left[(H \cdot \sin \Sigma)^2 + D^2 \right]^{1/2}}{2 \cdot H} \quad (13)$$

3) Reflected component

The view factor to unshaded ground of the front side of the collector *B* is calculated based on equation (9) and Fig. 2

$$L_1 = CD = H$$

$$L_2 = FD = H \cdot \cos \Sigma + D - S$$

$$L_3 = CF = \left[(H \cdot \cos \Sigma + D - S + H \cdot \cos \Sigma)^2 + (H \cdot \sin \Sigma)^2 \right]^{1/2}$$

from which it follows that

$$F_{B \rightarrow grd.us}^f = \frac{H \cdot (1 + \cos \Sigma) + D - S}{2 \cdot H} - \frac{\left[(D - S + 2 \cdot H \cdot \cos \Sigma)^2 + (H \cdot \sin \Sigma)^2 \right]^{1/2}}{2 \cdot H} \quad (14)$$

The view factor to shaded ground of the front side of the collector *B* is calculated based on equation (9) and Fig. 2

$$DF = H \cdot \cos \Sigma + D - S$$

$$DE = H \cdot \cos \Sigma + D$$

$$CF = \left[(H \cdot \cos \Sigma + H \cdot \cos \Sigma + D - S)^2 + (H \cdot \sin \Sigma)^2 \right]^{1/2}$$

$$CE = \left[(H \cdot \cos \Sigma + D + H \cdot \cos \Sigma)^2 + (H \cdot \sin \Sigma)^2 \right]^{1/2}$$

from which it follows that

$$F_{B \rightarrow grd.s}^f = \frac{\left[(H \cdot \cos \Sigma + H \cdot \cos \Sigma + D - S)^2 + (H \cdot \sin \Sigma)^2 \right]^{1/2}}{2 \cdot H} - \frac{\left[(H \cdot \cos \Sigma + D + H \cdot \cos \Sigma)^2 + (H \cdot \sin \Sigma)^2 \right]^{1/2} + S}{2 \cdot H} \quad (15)$$

E. View Factors for the Rear Side of the Modules

1) Direct component

Since just a small fraction of direct irradiation comes to the rear side of bifacial inclined modules, the view factor will not be taken into account when calculating the direct irradiation component to the rear side of the module.

2) Diffuse component

The view factor of the rear side of collector *B* to the sky is determined based on equation (8) and Fig. 2, so that the following expression is obtained

$$F_{B \rightarrow sky}^r = \frac{H + D + H \cdot \cos \Sigma}{2 \cdot H} - \frac{\left[(D + 2 \cdot H \cdot \cos \Sigma)^2 + (H \cdot \sin \Sigma)^2 \right]^{1/2}}{2 \cdot H} \quad (16)$$

3) Reflected component

The view factor of the rear side of collector *B* to unshaded part of the ground is determined based on equation (9) and Fig. 2, so that the following expression is obtained

$$F_{B \rightarrow grd.us}^r = \frac{\left[(S - H \cdot \cos \Sigma)^2 + (H \cdot \sin \Sigma)^2 \right]^{1/2}}{2 \cdot H} + \frac{H \cdot \cos \Sigma + D - \left[D^2 + (H \cdot \sin \Sigma)^2 \right]^{1/2} - S}{2 \cdot H} \quad (17)$$

The view factor of the rear side of collector *B* to shaded part of the ground is determined based on equation (9) and Fig. 2, so that the following expression is obtained

$$F_{B \rightarrow grd.s}^r = \frac{H + S}{2 \cdot H} - \frac{\left[(S - H \cdot \cos \Sigma)^2 + (H \cdot \sin \Sigma)^2 \right]^{1/2}}{2 \cdot H} \quad (18)$$

After calculating all required view factors, the total irradiation on bifacial PV modules is determined by using equation (7). Front-side irradiation is obtained directly from the equation. In order to calculate the rear-side irradiation, the module tilt angle Σ is increased by 180° which actually simulates a rotation of the module around its axis.

F. Calculating the AC Power Output

The conversion from the available irradiance to the generated AC power is done in three steps. In the first step, based on the irradiation *G*, theoretical maximum DC power at the connections of the photovoltaic modules P_{DC} is estimated. This conversion is mathematically modeled using the following expression [22]

$$P_{DC} = \frac{G}{1000} \cdot P_{DC0} \cdot (1 + \gamma \cdot (T_c - 25)) \quad (19)$$

where P_{DC0} is the nameplate DC rating of the PV modules given by the manufacturer for the reference cell temperature $T_{ref} = 25^\circ\text{C}$ and reference irradiance 1000 W/m^2 , γ is the temperature coefficient of the output power and T_c is the cell temperature.

The cell temperature is estimated by the so-called Nominal Operating Cell Temperature (NOCT) model, which is defined by IEC standards [15]

$$T_c = T_{amb} + \frac{G}{800 \text{ W/m}^2} \cdot (NOCT - 20^\circ\text{C}) \quad (20)$$

where T_{amb} is the ambient temperature and G is the total irradiance falling on both sides of the modules, while $NOCT$ is the nominal operating cell temperature in $^\circ\text{C}$ which is usually provided by the manufacturer of the PV module, observed under the reference conditions (module exposed to 800 W/m^2 irradiation at 20°C ambient temperature and with wind velocity of about 1 m/s). It is noticed from equation (20) that the cell temperature estimated by using $NOCT$ model does not take into account the changes in actual wind velocity.

Theoretical maximum power output P_{DC} cannot be achieved in reality due to unavoidable difficulties such as module mismatch, soiling, wiring and connection losses, light induced degradation, etc. These losses are estimated to 11% in total [22]. If we denote the loss factor by k_{loss} , the DC power supplied to the inverter input will be

$$P'_{DC} = (1 - k_{loss}) \cdot P_{DC} \quad (21)$$

Finally, the inverter losses should be accounted for, in order to determine the AC power delivered to the grid. There are several approaches for modeling the inverter efficiency in terms of its power output. However, since the number of inverters in the system and detailed connection configuration are not specified in such a planning problem, a simple model based on the average inverter efficiency η_{inv} was employed in this paper

$$P_{AC} = \eta_{inv} \cdot P'_{DC} \quad (22)$$

IV. NUMERICAL RESULTS

All required models are implemented by MATLAB/Octave scripts and the software is tested by drawing some illustrative charts. The tests are performed on the monofacial and bifacial PV modules located at 44.77° N latitude (Banja Luka, Bosnia and Herzegovina). The modules are 2 m long and have south orientation ($\Phi_C = 0^\circ$). Reflection coefficient is assumed to be 0.25 , which is a typical value for the soil covered with grass. The input data for irradiation and ambient temperature are Typical Meteorological Year (TMY) hourly time series loaded from PVWatts online calculator.

A. Optimum Tilt Angle

By varying the tilt angle from 20° to 50° , the optimum value for maximum annual energy production can be found. The optimum tilt angles obtained for the test systems located in Banja Luka are 30° for monofacial and 44° for bifacial modules. When determining the optimal angles, it is assumed that the distance between the rows of PV modules are large enough to avoid self-shading. The dependence of the irradiation of monofacial and bifacial PV modules on the tilt angle is shown in Fig. 5 and 6, respectively. The obtained results confirm the expectations, that the optimal tilt angle of bifacial PV modules is larger than the optimal tilt angle of monofacial PV modules.

For multi-row bifacial PV power plants, the optimal tilt angle generally increases with the size of the system [23]. As the number of modules increases, the surface area of the

shadow becomes larger and in order to reduce the self-shading effect and collect more radiation, the tilt angle must be enlarged. Bifacial modules with a small tilt angle "see" a large part of their own shadow, and by increasing the tilt angle, the back of the module receives more radiation from the ground and sky and less from the shaded area. Unlike bifacial modules, the optimal tilt of monofacial modules does not depend to a large extent on the size of the system.

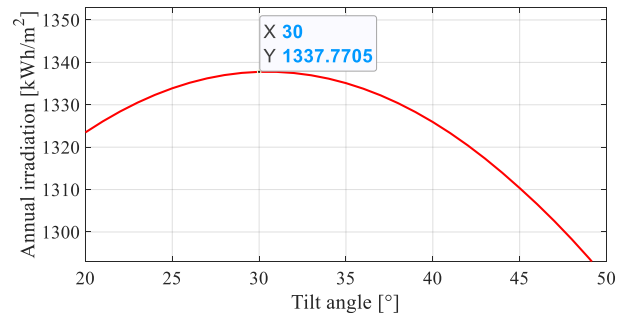


Figure 5. Annual irradiation to monofacial modules as a function of tilt angle

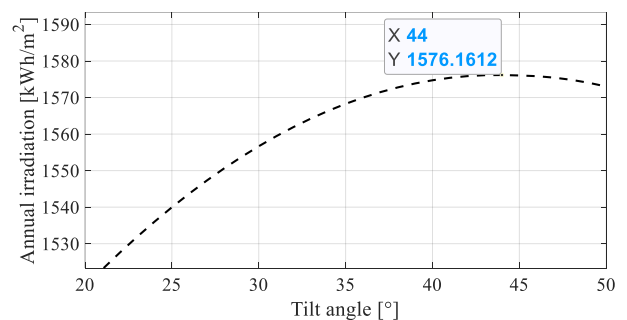


Figure 6. Annual irradiation to bifacial modules as a function of tilt angle

B. Distance Between the Rows

In order to determine the optimal distance between the rows of monofacial and bifacial modules, the simulations are performed assuming that the tilt angles are set to the optimal values of 30° and 44° , respectively. Fig. 7 shows the annual irradiation to the modules as a function of the distance between the rows. It can be noticed that the irradiation to the modules at small distances largely depends on the distance between the rows, while at larger distances it slowly asymptotically approaches a constant value. The theoretical optimum distance clearly tends to infinity when the limitation of the available plot area is not taken into account. On the other hand, the realistic optimal distance was chosen by engineering judgment as a compromise between the minimum shading in the period from 9 am to 5 pm and the minimum area of occupied land. As shown in Fig. 7, the recommended distances between the rows for monofacial and bifacial modules are set to 3 m and 4 m , respectively.

C. Influence of Albedo

Several simulations are performed in order to analyze the impact of ground albedo to the performance of PV systems. Albedo (ground reflection coefficient ρ) is varied from 0 to 1, while the tilt angle and distance between rows are set to their optimal values, as determined in sections IVA and IVB.

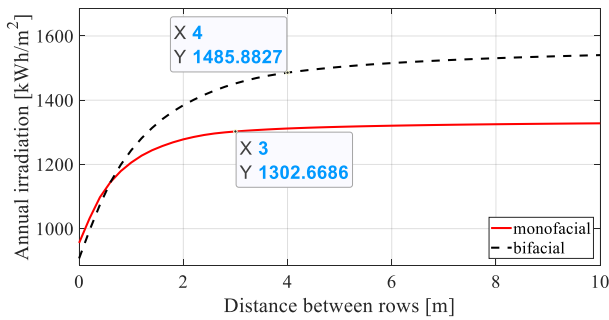


Figure 7. Annual irradiation on monofacial and bifacial PV modules as a function of distance between the rows

It can be noticed from Fig. 8 that irradiation of bifacial PV modules increases significantly with growth of albedo, following a linear trend. The influence of albedo on monofacial PV modules is rather small since the effect of reflected radiation on the front side of the panel is significantly less than on the rear side. A higher albedo generally leads also to a higher optimal tilt angle because the modules receive more radiation reflected from the ground at both the front side and rear side, when the tilt angle is increased.

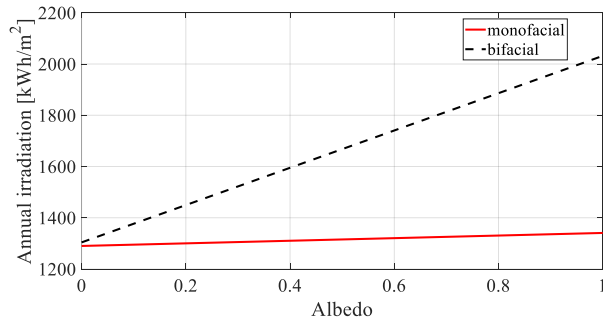


Figure 8. Annual irradiation on bifacial PV modules as a function of albedo

D. Monthly Distribution of Irradiation

In the next set of simulations, the distribution of produced energy by particular months was examined. The optimal values of input parameters determined in the previous sections were used in these simulations. Fig. 9, 10 and 11 show the values of direct, diffuse and reflected radiation on PV modules, respectively. Fig. 12 shows the total radiation to PV modules, computed as the sum of all three above mentioned components. The total annual radiation under optimal installation conditions is 1303 kWh/m² for monofacial PV modules and 1486 kWh/m² for bifacial PV modules. It is concluded that the bifacial PV modules under optimal mounting conditions receive 14.04% higher irradiation in comparison to their monofacial counterpart.

E. AC Energy Output

Once the irradiation for each type of PV installation is determined, the possible AC electricity output of the system can be calculated. The simulation is performed by using 450 Wp PV modules, monofacial with 20.70% efficiency and bifacial with 20.38% efficiency. The AC power output is determined by using equations (19) - (22). Average inverter efficiency is assumed to be 98% while the total other losses are

set to 11%. Fig. 13 shows the monthly values of generated energy as measured on the AC side of the inverter.

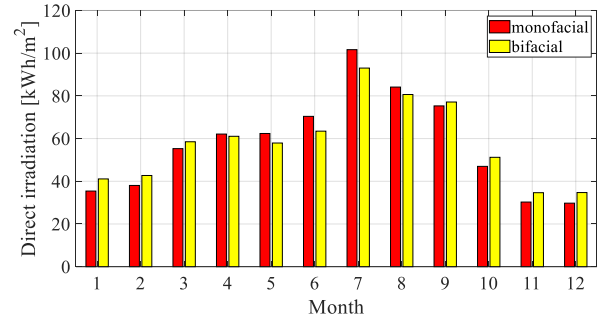


Figure 9. Direct irradiation on PV modules

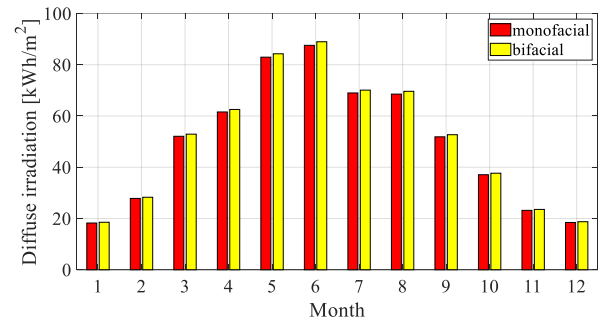


Figure 10. Diffuse irradiation on PV modules

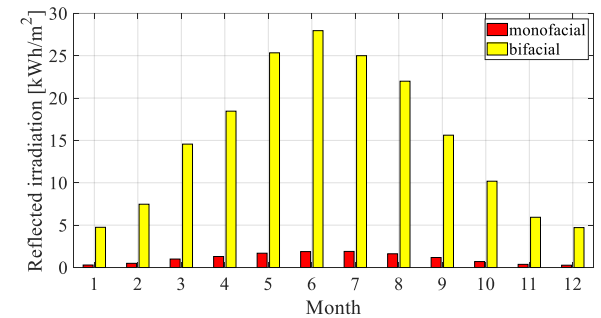


Figure 11. Reflected irradiation on PV modules

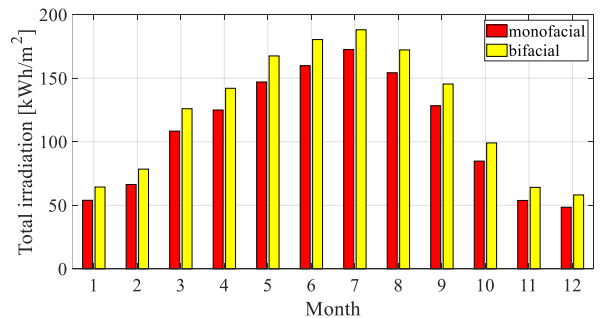


Figure 12. Total irradiation on PV modules

The observed monofacial PV modules have the potential to produce 494 kWh, while the bifacial PV modules are capable of generating 567 kWh, each under their optimal installation conditions. It is concluded that the bifacial PV modules would

produce 14.78% more electricity in comparison to monofacial PV modules.

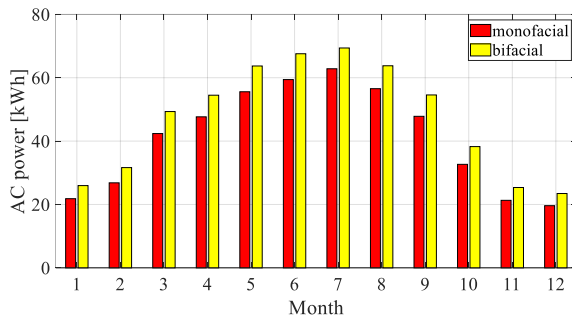


Figure 13. System AC energy output

F. Comparison of Simulation Results with the Results Provided by Online Calculators

The simulation results were compared with the results provided by two characteristic online calculators, namely PVWatts [19] and nanoHUB calculator [24]. The results of the monofacial PV model are compared with the results of the PVWatts calculator, while the results of the bifacial PV model are compared with the results of the nanoHUB calculator. The reason for using both calculators is that the PVWatts calculator does not implement bifacial PV modules, while on the other hand the nanoHUB calculator was the only freely available online calculator which incorporates model of bifacial PV modules. The comparison of the results is shown in Table I.

TABLE I. COMPARISON BETWEEN THE SIMULATION RESULTS AND RESULTS OBTAINED BY ONLINE CALCULATORS

Month	Irradiation (kWh/m ²)			
	Monofacial		Bifacial	
	PVWatts calculator	Employed model	nanoHUB calculator	Employed model
1	59.83	53.95	65.93	64.37
2	72.24	66.37	94.01	78.46
3	119.35	108.36	131.65	125.98
4	134.40	124.97	138.60	142.06
5	155.93	147.02	170.68	167.52
6	168.90	159.85	172.34	180.39
7	180.73	172.51	189.94	188.09
8	164.92	154.27	180.50	172.24
9	140.70	128.34	141.94	145.42
10	93.31	84.75	99.40	99.07
11	61.20	53.81	55.08	64.12
12	55.80	48.47	49.33	58.16
Avg.	117.28	108.56	124.12	123.82

For monofacial modules, the PVWatts online calculator gives results that are 8% higher on the annual level when compared to the results of the model used in this paper. We expect that the main reason for this difference is that the online calculator employs the Perez model to calculate the diffuse irradiance, while the isotropic model is used in this paper. The results for the bifacial models obtained using the nanoHUB

calculator and the model used in this paper are almost identical on the annual level. A certain difference that exists in the distribution by individual months is a consequence of different input data used for irradiation. The nanoHUB calculations are based on TMY data obtained from NASA meteorological database which are similar but not identical to TMY data used by the PVWatts calculator.

V. CONCLUSION

This paper shows that it is possible to create a relatively simple software tool for estimating the annual energy output of bifacial photovoltaic plants. Using the developed simulation platform, influence of several important input parameters is investigated, including the module tilt angle, the distance between the rows and the ground albedo. The simulations proved that, in order to achieve the highest energy yield, modules should be installed at the location of the highest possible albedo, and the distance between the rows should be large enough so that the effects of self-shading and the influence of the adjacent modules are minimal. Input data for the presented framework is the Typical Meteorological Year so that one of the directions for further work will be the software upgrade towards the simulation using artificially generated hourly time series for probabilistic analysis. It must be noted that the module elevation above the ground is considered to be zero both in the models and simulations given in this paper. Testing the influence of mounting height on the performance of bifacial PV systems is also left for the future work.

REFERENCES

- [1] REN21 Secretariat, "Renewables 2020 Global Status Report," Tech. Rep. ISBN 978-3-948393-00-7, Paris, 2020.
- [2] L. Dias, J. P. Gouveia, P. Lourenço, and J. Seixas, "Interplay between the potential of photovoltaic systems and agricultural land use," *Land Use Policy*, vol. 81, pp. 725–735, Feb. 2019.
- [3] Eduardo Lorenzo, "On the historical origins of bifacial PV modelling," *Solar Energy*, vol. 218, 5, Apr. 2021.
- [4] N. Ishikawa, "World First Large Scale 1.25MW Bifacial PV Power Plant on Snowy Area in Japan," 3rd bifi PV workshop in Miyazaki, Japan, Sep. 2016.
- [5] VDMA, "International Technology Roadmap for Photovoltaic (ITRPV): 2019 Results," Eleventh Edition, April 2020, [Online]. Available: <http://www.itrpv.net/Reports/Downloads/>
- [6] A. Cuevas, A. Luque, J. Eguren, and J. del Alamo, "50 Percent more output power from an albedo-collecting flat panel using bifacial solar cells," *Solar Energy*, vol. 29, pp. 419–420, 1982.
- [7] J. Appelbaum, "Bifacial photovoltaic panels field," *Renewable Energy*, vol. 85, pp. 338–343, Jan. 2016.
- [8] J. Appelbaum, "The role of view factors in solar photovoltaic fields," *Renewable and Sustainable Energy Reviews*, vol. 81, pp. 161–171, Jan. 2018.
- [9] V. Durković and Ž. Đurišić, "Extended model for irradiation suitable for large bifacial PV power plants," *Solar Energy*, vol. 191, pp. 272–290, Oct. 2019.
- [10] D. Chudinow, J. Haas, G. Díaz-Ferrán, S. Moreno-Leiva, and L. Eltrop, "Simulating the energy yield of a bifacial photovoltaic power plant," *Solar Energy*, vol. 183, pp. 812–822, May 2019.
- [11] X. Sun, M. R. Khan, C. Deline, and M. A. Alam, "Optimization and performance of bifacial solar modules: A global perspective," *Applied Energy*, vol. 212, pp. 1601–1610, Feb. 2018.
- [12] I. Shoukry, J. Libal, R. Kopecek, E. Wefringhaus, and J. Werner, "Modelling of bifacial gain for stand-alone and in-field installed bifacial PV modules," *Energy Procedia*, vol. 96, pp. 600–608, Aug. 2016.

- [13] W. Gu, T. Ma, S. Ahmed, Y. Zhang, and J. Peng, "A comprehensive review and outlook of bifacial photovoltaic (bPV) technology," *Energy Conversion and Management*, vol. 223, article no. 113283, Nov. 2020.
- [14] Sandia National Laboratories, "Sandia Module Temperature Model," [Online]. Available: <https://pvpmc.sandia.gov/modeling-steps/2-dc-module-iv/module-temperature/sandia-module-temperature-model/>
- [15] International Electrotechnical Commission, "Crystalline Silicon Terrestrial Photovoltaic (PV) Modules - Design Qualification and Type Approval," IEC 61215:2005, 2005.
- [16] D. Faiman, "Assessing the outdoor operating temperature of photovoltaic modules," *Progress in Photovoltaics: Research and Applications*, vol. 16, pp. 307–315, June 2008.
- [17] U. A. Yusufoglu, T. M. Pletzer, L. J. Koduvelikulathu, C. Comparotto, R. Kopecek, and H. Kurz, "Analysis of the Annual Performance of Bifacial Modules and Optimization Methods," *IEEE Journal of Photovoltaics*, vol. 5, no. 1, pp. 320–328, Jan. 2015.
- [18] T. S. Liang, M. Pravettoni, C. Deline, J. S. Stein, R. Kopecek, J. P. Singh, W. Luo, Y. Wang, A. G. Aberle, and Y. S. Khoo, "A review of crystalline silicon bifacial photovoltaic performance characterisation and simulation," *Energy & Environmental Science*, vol. 12, pp. 116–148, Jan. 2019.
- [19] National Renewable Energy Laboratory (NREL), PVWatts Calculator, [Online]. Available: <https://pvwatts.nrel.gov/>.
- [20] G. M. Masters, "Renewable and Efficient Electric Power Systems," New York: Wiley Interscience, 2004.
- [21] J. A. Duffie and W. A. Beckman, "Solar engineering of thermal processes," 4th edition, Hoboken: John Wiley & Sons, 2013.
- [22] A. P. Dobos, "PVWatts version 5 manual," National Renewable Energy Laboratory, Tech. Rep. NREL/TP-6A20-62641, September 2014.
- [23] A. Asgharzadehet, B. Marion, C. Deline, C. Hansen, J. S. Stein, and F. Toor, "A sensitivity study of the impact of installation parameters and system configuration on the performance of bifacial PV arrays," *IEEE Journal of Photovoltaics*, vol. 8, no. 3, pp. 798–805, May 2018.
- [24] Purdue University Bifacial Module Calculator (PUB), [Online]. Available: <https://nanohub.org/tools/pub/>



Nikola Ostojić received the B.Sc. (Dipl. Eng.) degree in electrical engineering from the University of Banja Luka, Bosnia and Herzegovina, in 2018. He is currently pursuing his master thesis at the University of Banja Luka, Faculty of Electrical Engineering. His work focuses on the modeling and simulation of photovoltaic systems.



Čedomir Zeljković received the B.Sc. (Dipl. Eng.) degree from the University of Banja Luka, Bosnia and Herzegovina, in 2003, and the M.Sc. and Ph.D. degrees from the University of Belgrade, Serbia, in 2008 and 2013, respectively, all in electrical engineering. He is currently an Associate Professor with the Faculty of Electrical Engineering, University of Banja Luka. His main areas of scientific interests are distributed generation and renewable sources in a power system, as well as the power network calculations and optimization.



Predrag Mršić received the B.Sc. and M.Sc. degrees in electrical engineering from the University of Banja Luka, Republic of Srpska, Bosnia and Herzegovina, in 2013 and 2017, respectively. He is currently working toward the Ph.D. degree with the University of Belgrade, Serbia. Currently, he is a Senior Teaching Assistant with the University of Banja Luka. His research interests include distribution automation, renewable energy sources, and power system reliability.